

Hydrogen storage properties of $Ml_{1-x}Ca_xNi_5$ pseudobinary intermetallic compounds

Xinhua Wang, Changpin Chen, Chunsheng Wang, Qidong Wang

Department of Materials Science and Engineering, Zhejiang University, Hongzhou, 310027, People's Republic of China

Received 22 March 1995; received in final form 29 May 1995

Abstract

The hydrogen storage properties of the pseudobinary intermetallic compounds $Ml_{1-x}Ca_xNi_5$ (where Ml is La-rich mischmetal and x varies from 0 to 0.9) were investigated over the temperature range of 25–80°C. It was found in experiment that with increasing x in $Ml_{1-x}Ca_xNi_5$ the incubation time for its first hydrogenation shortened, the first hydrogen absorption rate accelerated, the hysteresis lowered, and the dissociation pressure of the hydrides (25°C) increased when $x < 0.3$ but decreased in the range of $x = 0.3$ to 0.9. Considering the effect of the geometrical and electric factors, we deduced an equation for the dissociation pressure as a function of Ca content x . The equation agrees well with the test results.

Owing to the lower cost and favourable properties of $Ml_{0.8}Ca_{0.2}Ni_5$, a metal hydride container of 30 N m³ hydrogen capacity was designed and built to supply hydrogen for the hydrogen–gasoline hybrid fuel for an automobile engine.

Keywords: Hydride; Hydrogen storage properties; Hydrogen storage alloy; Intermetallic compound

1. Introduction

Since the discovery of hydrogen storage alloys, their applications have been frustrated to a large extent by their costs. Therefore, great efforts have been made not only to improve their properties but also to lower their costs. The development of $MmNi_5$ (Mm is Ce-rich mischmetal) and $MlNi_5$ (Ml is La-rich mischmetal) and Sandrock's investigation [1] on $Mm_{1-x}Ca_xNi_5$ family were typical examples. The studies on $Mm_{1-x}Ca_xNi_5$ and $La_{1-x}Ca_xNi_5$ families were also reported by Osumi et al. [2] and Shinar et al. [3] respectively. Sandrock's results show that the hydride dissociation pressure decreased with increasing Ca content x , while Osumi and Shinar's results indicate that the substitution of Ca for Mm or La caused an increase in hydride dissociation pressure. However, neither of them has quantitatively explained the mechanism of Ca substitution on the hydride dissociation pressure.

Owing to the excellent characteristics of $MlNi_5$ [4,5], including large hydrogen storage capacity, easy activation, low hysteresis, and strong resistance to poisoning, we investigated the properties of $Ml_{1-x}Ca_xNi_5$ ($x = 0.1, 0.2, 0.3, 0.5, 0.7, 0.9$) sys-

tematically in order to further improve its properties, lower its cost and to widen its applications. Based on the effect of geometrical factor (cell volume) and electric factor (element valence), we also deduced an equation for the dependence of the hydride dissociation pressure on Ca content x for the $Ml_{1-x}Ca_xNi_5$ family. The equation agreed with the test results very well.

In addition, in our laboratory we designed and built a metal hydride container of 30 N m³ hydrogen capacity with $Ml_{0.8}Ca_{0.2}Ni_5$ alloy to supply hydrogen for the hydrogen–gasoline hybrid fuel for an automobile.

2. Experimental details

The composition of Ml adopted in the test was 45.7% La, 2.8% Ce, 10.4% Pr, 40.1% Nd and 1% other rare earths. The metallic Ni was 99% pure, Ca 99% pure and the hydrogen 99.999% pure. Samples containing Ca were fabricated by two step melting. Firstly, Ml and Ca were melted into an intermediate alloy in an induction furnace under the protection of Ar. Then, the Ml –Ca alloy mixed with Ni was melted

Table 1
Alloy compositions

Designed composition	Actual composition
MI ₁ Ni ₅	MI ₁ Ni ₅
MI _{0.9} Ca _{0.9} Ni ₅	MI _{0.9} Ca _{0.99} Ni ₅
MI _{0.8} Ca _{0.2} Ni ₅	MI _{0.79} Ca _{0.19} Ni ₅
MI _{0.7} Ca _{0.3} Ni ₅	MI _{0.68} Ca _{0.31} Ni ₅
MI _{0.5} Ca _{0.5} Ni ₅	MI _{0.5} Ca _{0.48} Ni ₅
MI _{0.3} Ca _{0.7} Ni ₅	MI _{0.31} Ca _{0.69} Ni ₅
MI _{0.1} Ca _{0.9} Ni ₅	MI _{0.1} Ca _{0.91} Ni ₅

in an arc furnace under Ar atmosphere. MI₁Ni₅ sample was also prepared in an arc furnace. The chemical analysis results indicated that the actual compositions were close to its nominal ones as tabulated in Table 1.

The cell volumes of the alloys before hydrogenation were determined by X-ray diffraction measurements. The results revealed that all samples were nearly single phase with the CaCu₅ structure, and only a slight amount of (MI,Ca)₂Ni₇ phase was present in some samples.

All samples were crushed mechanically in air, then placed into a stainless steel reactor for characterization. The kinetic properties at the first hydriding process were measured under 30 atm hydrogen pressure at 25°C. All samples could be activated easily under the above conditions. The *p*-*c*-*T* plots were measured after several absorption-desorption cycles.

3. Results and discussion

3.1. The activation and absorption-desorption properties

The dynamic characteristics at the first hydriding process under 30 atm hydrogen pressure at 25°C are shown in Fig. 1. All the curves were apparently characterized by the kinetics of phase transition, and all samples could be activated easily, absorbing more than 90% of hydrogen within 1 h during the first hydriding process. The substitution of Ca for MI shortened the incubation time remarkably. When the Ca content *x* was increased, the incubation time shortened and the hydrogenation rate accelerated. This was probably because the surface of the alloy powder was modified and the outer atomic layers (maybe oxides) became more permeable to the hydrogen atoms due to the substitution of Ca for MI; hence the incubation time was shortened. Moreover, the substitution of MI by Ca might cause more nucleation sites to be available in the incipient period, resulting in the faster hydrogenation rate.

The test results also indicated that the hysteresis was decreased with increasing *x*, and when *x* < 0.3, only one plateau was observed in the *p*-*c*-*T* plots and the

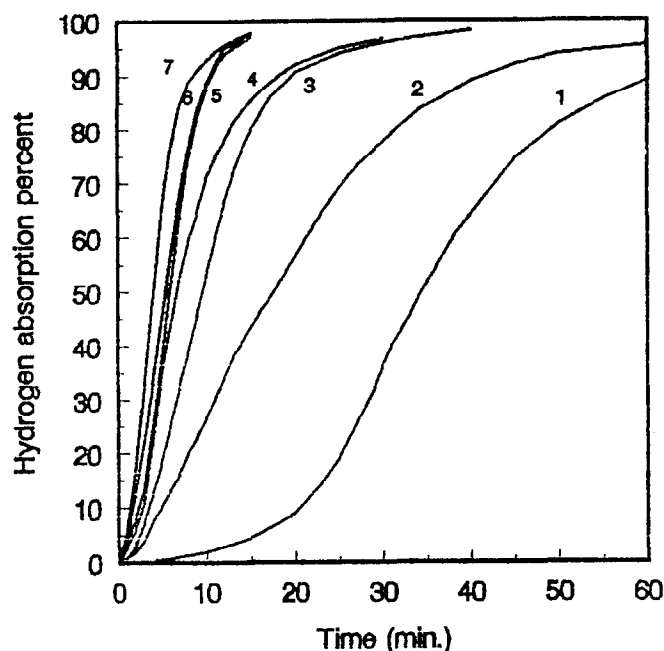


Fig. 1. The kinetic properties for the first hydriding process of the MI_{1-x}Ca_xNi₅ family: *x* = 0, 0.1, 0.2, 0.3, 0.5, 0.7, and 0.9 for curves 1–7 respectively.

plateau remained flat; in the range of *x* = 0.3–0.9 the *p*-*c*-*T* plots showed two plateaus which became steeper with increasing *x*, as shown in Fig. 2.

3.2. The relationship between the dissociation pressure and Ca content

Fig. 3 shows the test results of the hydride dissociation pressure versus Ca content *x*. At first, the replace-

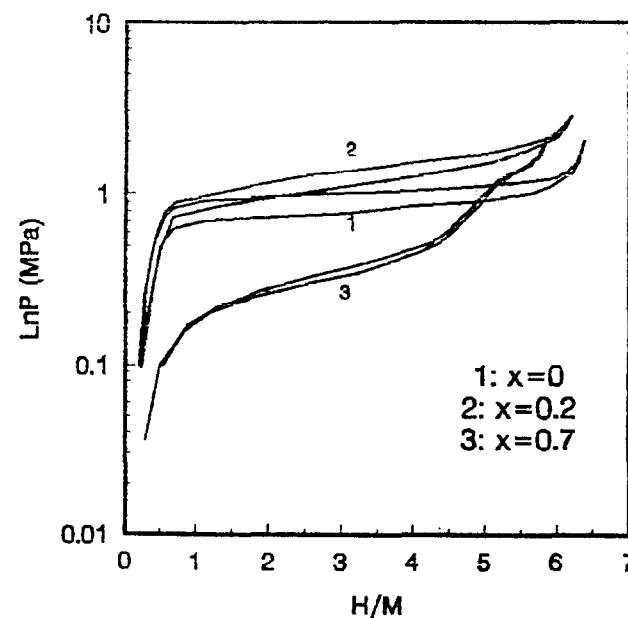


Fig. 2. The effect of Ca content *x* on the hysteresis and plateau pressure of MI_{1-x}Ca_xNi₅ alloys.

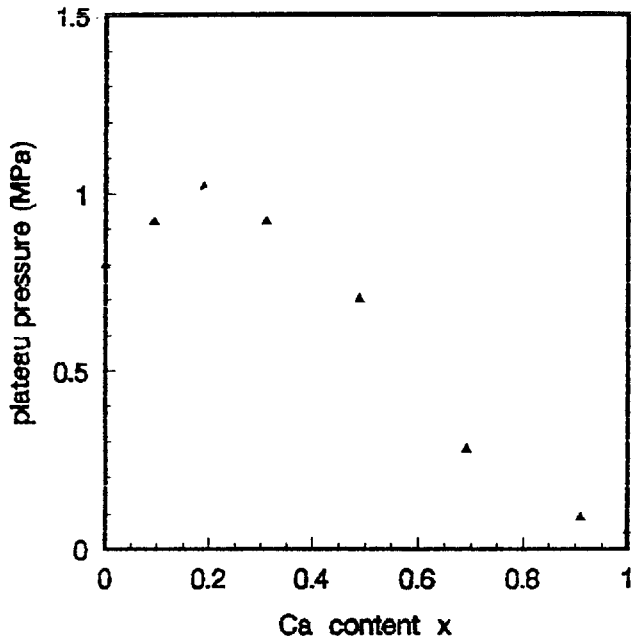


Fig. 3. Hydride dissociation pressure of $MI_{1-x}Ca_xNi_5$ intermetallic compounds.

ment of MI by Ca ($x < 0.3$) caused the hydrogen desorption equilibrium pressure to increase, while in the range of $x = 0.3$ to 0.9, the dissociation pressure decreased with increasing x . The cell volumes of the samples obtained from X-ray diffraction before hydrogenation decreased linearly with the Ca content x as shown in Fig. 4.

Some investigators had found that the correlation between dissociation pressure P and cell volume V of the hydride of $CaCu_5$ structure intermetallic com-

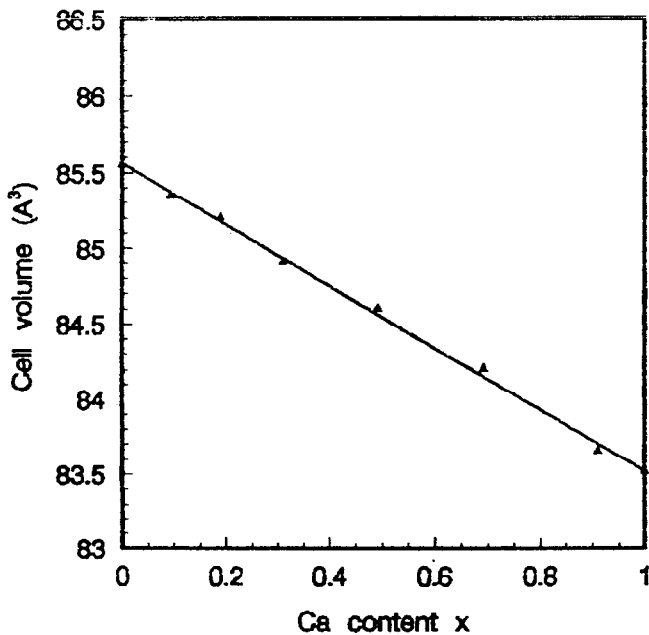


Fig. 4. Cell volume of $MI_{1-x}Ca_xNi_5$ intermetallic compounds.

pounds can be represented by the following equation [6,7]:

$$\ln P = (kV) + b \quad (1)$$

where P and V were dissociation pressure and cell volume respectively; k and b were constants with $k < 0$.

Fig. 5 shows the results for the pressure of RNi_5 ($R = Gd, Sm, Pr, Nd, La, Yb, Ca, MI$). The data for Gd, Sm, Pr, Nd, La, MI all fell on line 1, while those for Ca and Yb remarkably deviated from line 1. This phenomena is likely to be caused by the element valence difference. Ca and Yb are divalent elements, while the R elements which gave dissociation pressure and cell volume relation more closely associated with line 1 were trivalent. The deviation of Ca and Yb from line 1 indicated that the RNi_5 compounds with divalent R atoms showed a significantly lower dissociation pressure for the same cell volume than their corresponding trivalent R atom RNi_5 counterparts on line 1.

We regard the effect that the dissociation pressure decreased with increasing cell volume for the hydrides of trivalent R elements as the geometrical factor, and regard the deviation from line 1 caused by the different valence of R elements as the electric factor.

For the $MI_{1-x}Ca_xNi_5$ family, we made the following assumptions.

- (1) If the electric factor is ignored and only the geometric effect is considered, the dissociation pressure varies with cell volume according to line 1.

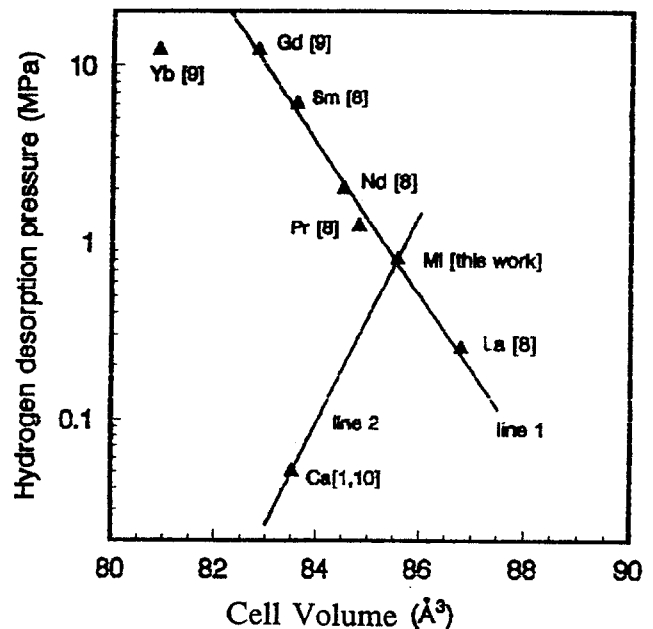


Fig. 5. Hydrogen desorption pressure (25°C) vs. cell volume compounds.

- (2) If the geometric effect is ignored and the electric factor alone is considered, the dissociation pressure varies with line 2, which is a line drawn from pressure/cell volume data of $M\text{Ni}_5$ to that of CaNi_5 .
- (3) For a real alloy when both the geometric factor and the electronic factor is considered, the effect of the geometric and electric factors should be in proportion to the content of M and Ca respectively.

In Fig. 5, the equations for line 1 and 2 can respectively be written as follows:

$$\ln P = k_1 V + b_1 \quad (2)$$

$$\ln P = k_2 V + b_2 \quad (3)$$

where k_1 , k_2 , b_1 and b_2 are constants with $k_1 < 0$ and $k_2 > 0$.

With the above assumptions, the hydride dissociation pressure for the $M\text{Ni}_{1-x}\text{Ca}_x\text{Ni}_5$ family can be given by

$$\ln P = (k_2 V + b_2)x + (k_1 V + b_1)(1-x) \quad (4)$$

where x is the mole fraction of Ca .

From Fig. 4., the equation for cell volume versus Ca content x was given by

$$V = k_3 x + b_3 \quad (5)$$

where k_3 and b_3 were constants with $k_3 < 0$.

Substituting Eq. (5) into Eq. (4) we obtain

$$\ln P = [k_1(k_3 x + b_3) + b_1](1-x) + [k_2(k_3 x + b_3) + b_2]x$$

then

$$\ln P = (k_2 k_3 - k_1 k_3)x^2 + (k_2 b_3 + b_1 + k_1 k_3 - k_1 b_3 - b_2)x + k_1 b_3 + b_2 \quad (6)$$

The constants k_i and b_i obtained from Figs. 4 and 5 are given in Table 2.

With the constants k_i and b_i substituted, Eq. (6) can be written as

$$\ln P = -1.1486x^2 + 195.5641x - 8322.0540 \quad (7)$$

$$P = \exp(-1.1486x^2 + 195.5641x - 8322.0540) \quad (8)$$

The theoretical curve together with the test results are shown in Fig. 6. This indicates that Eqs. (7) and (8) agreed with the test results very well.

Table 2

Constants k_i and b_i obtained from Figs. 4 and 5

k_1	k_2	k_3	b_1	b_2	b_3
-0.9840	1.3591	-2.0400	86.2731	-114.2060	85.5600

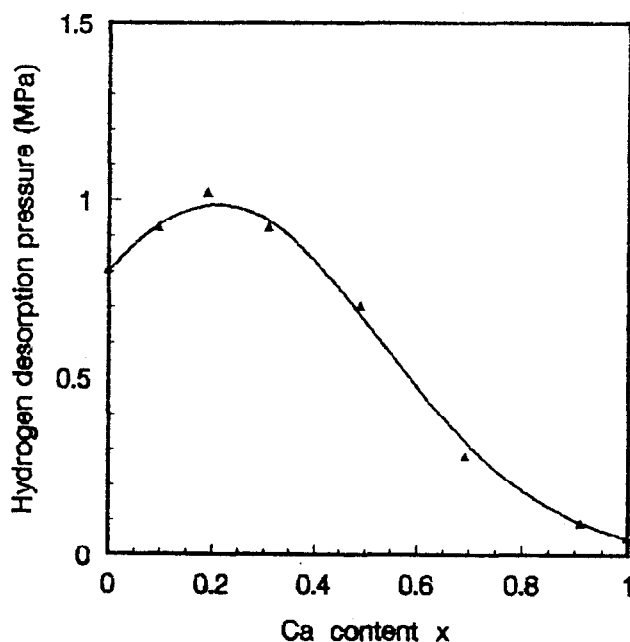


Fig. 6. The comparison of theoretical curve with the test results.

3.3. Example of application

Among the alloys tested, $M\text{Ni}_{0.8}\text{Ca}_{0.2}\text{Ni}_5$ had the most desirable properties. Its hydrogen storage capacity was up to 1.62 wt.% and its dissociation pressure and hysteresis (P_d/P_a) at 25°C were 10.2 atm and 1.25 respectively. It also has good kinetic characteristics and a flat plateau; Fig. 7 shows its p - c - T plots. It is a good alloy for hydrogen storage and transportation, hydrogen separation and purification. In our labora-

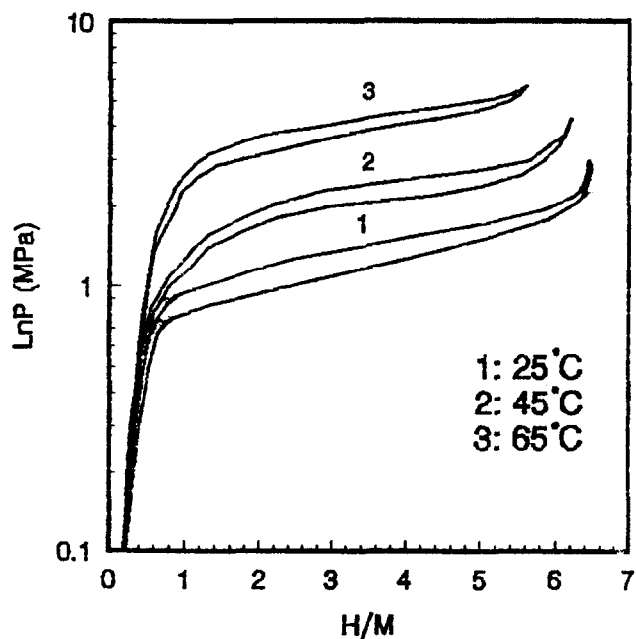


Fig. 7. The p - c - T plots for $M\text{Ni}_{0.8}\text{Ca}_{0.2}\text{Ni}_5$ -H system.

tory, a metal hydride container of 30 N m^3 hydrogen capacity was designed and built to supply hydrogen for the hydrogen and gasoline hybrid fuel for an automobile. The container consisted of 19 51 mm diameter stainless steel tubes, each 1.5 m long. $\text{Ml}_{0.8}\text{Ca}_{0.2}\text{Ni}_5$ was the alloy used. The special aluminium fibre was adopted to improve the heat and mass transfer as well as to eliminate the container deformation caused by hydrogenation expansion. The test results were quite satisfactory and will be reported elsewhere.

4. Conclusions

- (1) Compounds of the $\text{Ml}_{1-x}\text{Ca}_x\text{Ni}_5$ family could be activated easily under 30 atm hydrogen pressure at 25°C . The substitution of Ca for Ml shortened the incubation time remarkably and accelerated the hydrogenation rate.
- (2) Owing to the effect of geometrical and electric factors, the correlation between dissociation pressure and Ca content x for the $\text{Ml}_{1-x}\text{Ca}_x\text{Ni}_5$ family agreed well with the following equation

$$\ln P = -1.1486x^2 + 195.5641x - 8322.0540$$
- (3) $\text{Ml}_{0.8}\text{Ca}_{0.2}\text{Ni}_5$ has favourable hydrogen storage properties and is comparatively inexpensive. A metal hydride container of 30 N m^3 hydrogen capacity has been designed and built to supply hydrogen for the hydrogen and gasoline hybrid fuel for an automobile.

Acknowledgment

This project is financially supported by the National Advanced Science and Technology Foundation of China.

References

- [1] G.D. Sandrock, *Proc. 12th IECEC, Vol. 1*, American Nuclear Society, 1977, p. 951
- [2] Y. Osumi, H. Suzuki, A. Kato, M. Nakane and A. Miyake, *J. Chem. Soc. Jpn.*, 11 (1978) 1472.
- [3] J. Shinar, D. Shaltiel, D. Davidov and A. Grayevsky, *J. Less-Common Met.*, 60 (1978) 209.
- [4] Q.D. Wang, J. Wu and C.P. Chen, *Z. Phys. Chem. Neue Folge*, 164 (1989) S1293.
- [5] Q.D. Wang, J. Wu, C.P. Chen and T.S. Fang, *Rare Earth*, 3 (1984) (in Chinese).
- [6] M.H. Mendelsohn, D.M. Gmen and A.E. Dwight, *Nature*, 269 (1977) 19.
- [7] G. Busch, L. Schlapbach, A. Seiler, in A.F. Andresen and J.A. Maeland (eds.), *Hydrides for Energy Storage*, Pergamon, Oxford, 1978, p. 293.
- [8] F.A. Kuijpers, *Philips Res. Rept. Suppl.*, 2, (1973).
- [9] J.L. Anderson, T.C. Wallace, A.L. Bowman, C.L. Radosewich and M.L. Courtney, *Los Alamos Rep. LA-5320-MS*, 1973, University of California, NM.
- [10] W.B. Pearson, *A Handbook of Lattice Spacing and Structure of Metals and Alloys*, Vol. 2, Pergamon Press, Oxford, 1967.